
©2010 IEEE. Personal use of this material is permitted. However, permission to reprint/republish this material for advertising or promotional purposes or for creating new collective works for resale or redistribution to servers or lists, or to reuse any copyrighted component of this work in other works must be obtained from the IEEE.

Investigating PHEV Wind Balancing Capabilities using Heuristics and Model Predictive Control

Matthias D. Galus *Student Member, IEEE*, Raffael La Fauci *Student Member, IEEE*,
Göran Andersson, *Fellow, IEEE*

Abstract—The strive for sustainable energy systems will most likely lead to an increased use of renewable energy sources which to a large extent are fluctuating. Therefore, a larger demand for balancing capacity will be required to maintain system security. Plug-in Hybrid Electric Vehicles (PHEV) represent a potential storage which could offer additional balancing power. Here, the applicability of PHEVs for this purpose is investigated. The study is performed in a system including a wind farm. The PHEV storage management approaches are based on a heuristic- and on a model predictive control scheme. They are compared in case studies. It is shown that the heuristic scheme is scalable while both schemes are able to balance the forecast error of renewable sources to an acceptable level.

Index Terms—PHEV, V2G, balancing energy, MPC, wind power forecast, energy hub, heuristic

I. INTRODUCTION

The members of the EU decided in 2007 that 34% of electricity shall come from renewable generation by 2020 [1], [2]. The suggested sources are wind, solar, geothermal, hydropower, and others [3]. Although this goal is ambitious, the plan will certainly lead to a higher renewable energy production and subsequently to a larger stochastic component in power generation planning and operation [4]. Hence, the demand for balancing services ensuring system security will increase [5]. These services are costly and often, as in e.g. Germany, wind power producers are not obliged to contribute in bearing them. This is likely to change as [6] suggests participation schemes possibly affecting wind power producers competitiveness. Therefore, balancing the forecast error could become crucial.

Plug-In Hybrid Electric Vehicles (PHEVs) offer one possible source of balancing energy. These use mostly electric energy for propulsion and can be connected to the power grid in order to recharge their batteries [7]. These distributed and mobile batteries can be envisioned to both draw power from and feed power into the grid, the latter called V2G services [8]. Hence, they could be used as a possible storage for power systems. The storage persists while the PHEVs are connected to the grid. Acquisition costs of the PHEVs could be offset by offering balancing power at market prices possibly to wind power producers or other entities, possibly the Independent System Operator (ISO) or to Balance Group Responsibilities (BGR). A potential average income between 30€ and 80€ per PHEV per month was found [9].

The vehicles cannot independently offer their services as large storages of several MWs and hours are demanded by the bulk power system. An aggregator [10] could manage large number of cars. The entity would need to control its resources efficiently, depending on the balancing signal given by the system. So far, not much attention has been paid to the actual control of the individual cars in dependence of their own and the system objectives [11]. Here, a simple heuristic scheme is developed and validated via a comparison with model predictive control of each PHEV. The heuristic scheme offers the potential to be implemented in real time using wind forecasts. The next sections will introduce the system model, the balancing signal based on wind data, PHEVs as storage and the two control algorithms. Case studies are performed and a summary concludes the paper.

II. MODEL

The model consists of a power system including a wind power plant. The system is modelled by use of the energy hub approach. PHEVs are connecting only at one node for simplicity. Wind forecasts are used to plan and simulate the system power flow in the base case. The deviations from the forecast and the actual wind production are balanced by the PHEVs considering system constraints.

A. Energy hub system

The investigated system includes different energy carriers \mathcal{E} defined by (1) and a set of network nodes \mathcal{N} (2). Each node is represented by an energy hub (3). PHEVs, expressed through set (4), are assumed to connect throughout the day. The set of connected PHEVs is defined for each time interval t and consists of several subsets (5) which represent vehicles which are arriving (A), already parked (P) or departing (D) in t .

$$e, g, h \dots \in \mathcal{E} = \{\text{electricity, natural gas, hydrogen, } \dots\} \quad (1)$$

$$m, n, \dots \in \mathcal{N} = \{1, 2, \dots, N_N\} \quad (2)$$

$$i, j, \dots \in \mathcal{H} = \{1, 2, \dots, N_H\} \quad (3)$$

$$k_n, l_n \dots \in \mathcal{PHEV}_n(t) = \{1, 2, \dots, N_{PHEV_n}\} \quad (4)$$

where

$$\mathcal{PHEV}_n(t) = \mathcal{PHEV}_n^A(t) \cup \mathcal{PHEV}_n^P(t) \cup \mathcal{PHEV}_n^D(t) \quad (5)$$

The complete system is depicted in figure 1. It consists of four interconnected hybrid energy hubs. The system could be understood to model urban agglomerations within a balance group. The urban areas are partly supplied by infeeds from higher network levels and by a wind generation plant. PHEVs

are presumed only to be connecting to node 2. A hub includes conversion of input energy carriers for a certain area to supply its loads. Here, electricity and natural gas are fed into the hub at the input side and are converted to supply electricity demand on a lower voltage level and heat. Since electric power can be produced by using natural gas through, for instance, CHP turbines, the electricity and gas networks are linked which results in a hybrid system. See [12] for a general discussion of interconnected hub networks.

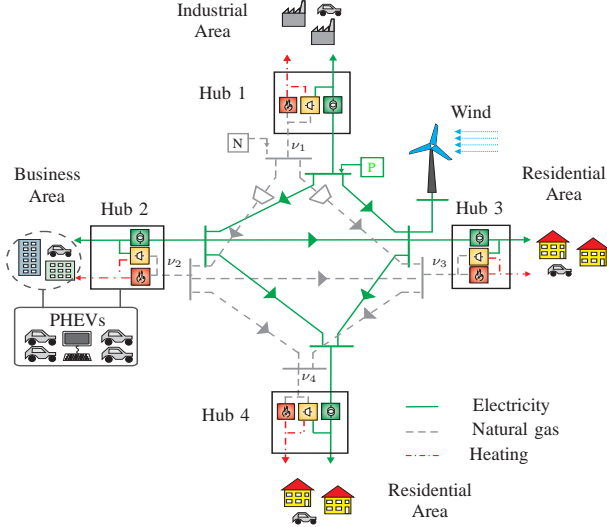


Fig. 1: 4 Hub network including wind generator

In equation (6), the hubs are specified. It models a transformer, a CHP and a furnace within each hub. The input powers are given by P and the output by L . The electricity and gas input powers are denoted by e and g . The output powers, electricity and heat, are given by e and h . The time step is denoted with t and is important in optimization schemes presented in II-E. The variable ν denotes the dispatch factor. It is used to determine the fraction of natural gas flowing into the CHP and the furnace, respectively. The coupling factors in the coupling matrix C contain the efficiencies of all conversions in one power path. The transformer efficiency is denoted by η_{ee}^{TR} while η_{ge}^{CHP} and η_{gh}^{CHP} are used for the CHP.

$$\underbrace{\begin{bmatrix} L_e(t) \\ L_h(t) \end{bmatrix}}_L = \underbrace{\begin{bmatrix} \eta_{ee}^{TR} & \nu_g(t)\eta_{ge}^{CHP} \\ 0 & \nu_g(t)\eta_{gh}^{CHP} + (1 - \nu_g(t))\eta_{gh}^F \end{bmatrix}}_C \underbrace{\begin{bmatrix} P_e(t) \\ P_g(t) \end{bmatrix}}_P \quad (6)$$

B. Power transmission

The electric power flows are computed by a DC power flow [13] for simplicity. The gas power flow is derived from a physical model including upstream and downstream pressures, compressors and pipeline constants for the gas streams. The exact formulations for the complete network models are found in [12], [14]. Grid constraints were introduced to visualize the applicability of the model though the focus of the paper is on the PHEVs and their management.

C. Integration of a wind farm

Wind forecasts are used for power production planning typically performed by BGRs. In Switzerland two forecasts are available, officially published by the Federal Office of Meteorology and Climatology in Switzerland, backed by the Consortium for Small-Scale Modeling (COSMO). The available forecasts facilitate numerical weather prediction models with equations, based on physical laws, modelling the weather behavior [15]. Both forecasts use a geographical grid. COSMO-7 uses a spacing of 6.6 km, considers Central and Western Europe and predicts the weather for the next 72 hours. COSMO-7 is published twice a day, at 01:45 a.m. and 01:45 p.m. winter time. COSMO-2 uses a 2.2 km spacing and offers a 24-hour forecast. It is published, i.e. updated, every three hours beginning at 01:45 a.m. winter time [16]. The smaller spacing allows for a more accurate forecast.

In electricity markets bids for day ahead production typically have to be submitted until 10:30 a.m. An example on how production schedules could be planned with the COSMO forecasts is given in figure 2. The graph shows the wind power production forecast using COSMO-7. Here, the day ahead schedule 11:00 a.m. (hour 34) to 8:00 a.m. (hour 56) needs to be submitted. As can be seen, the forecast range of COSMO-2 is too small. The more accurate COSMO-2 cannot be used for day ahead planning. Hence, the imprecise COSMO-7 needs to be utilized introducing a potential larger error.

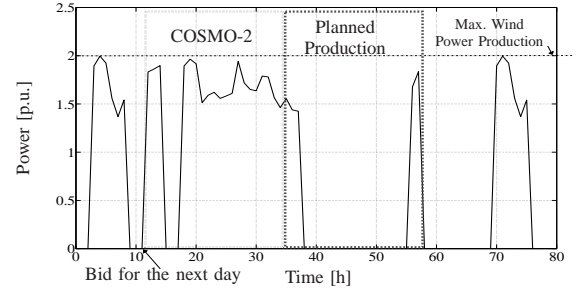


Fig. 2: Planning of wind power production

In the model, the produced wind power depends on the wind speed according to a simplified but nonlinear model [13]. Minimal wind speeds are needed for production. Between minimal and maximal turbine output power, the wind power depends nonlinearly on the speed. After the maximal output power is reached, production saturates at a constant level. Upon reaching the upper limit for wind speed, the turbine is shut down. Here, the maximal wind power is defined to be 2 p.u. Figure 3 exemplifies forecast deviations from the real wind production ($P_{w,n}^R$) at node n , displayed by the black graph. The grey graph shows COSMO-2 ($P_{w,n}^{\Gamma 2}$) whereas the dashed grey graph denotes the COSMO-7 ($P_{w,n}^{\Gamma 1}$) power production forecast. The dotted horizontal line denotes the maximal wind power production. As expected, the COSMO-2 forecast is more accurate. The difference between forecast and real production can be substantial for large shares of wind power and needs to be balanced. Clearly, for fluctuating generation aggregated over a large area the error might be

smaller. However, with rising wind power shares ancillary services such as primary-, secondary- and tertiary- control power introduce high costs [17] and hence create an opportunity for PHEVs to profit by supplying parts of these services.

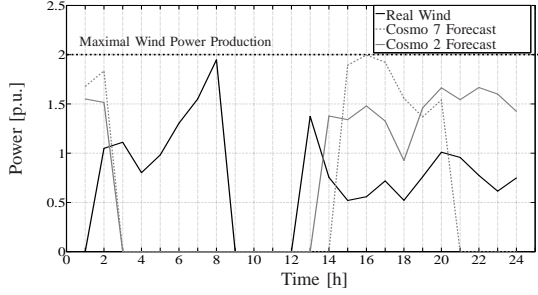


Fig. 3: Example: wind forecast and real power production

D. PHEVs as energy storage devices

The PHEVs in this study are all presumed to include a 3.5 kW connection and are used for system services only. Charging and discharging are considered to be free of costs, i.e. the PHEVs do not need to pay for received energy since they provide a service. Individual recharging demands are neglected under the presumption of PHEVs being contracted only for ancillary services and compensated for the disadvantage not to be recharged individually. This is based on the fact that PHEVs can utilize their combustion engine if their battery should be depleted. The connection area (i.e. hub 2) is assumed to include smart interface devices providing information about arrival and departure times as well as individual state of charge (SOC) [18].

The hub at which the PHEVs are connecting represents an area dominated by commercial customers. Hence, vehicle presence is assumed to be according to figure 4. Availability during night is neglected. Arrival and departure times as well as their SOC at arrival were individually simulated by the model described in [19]. The SOC lies between 20% and 100% and battery capacities are 10 kWh. The availability, though simplified, is consistent with earlier findings showing that most secondary cars in Germany are parked at the working location from approximately 6:00 a.m. until 6:00 p.m. [20]. Balancing power can only be offered during this time frame. In figure 4 the dashed black line denotes the evolution of total available PHEV storage (in MWh) while the black bars show available feedback power (in MW) for secondary reserve. The dashed grey line and the grey bars show total demand and maximal loading power, respectively. The presumed maximal duration for balancing services i.e. secondary control reserve, is one hour.

The time steps in figure 4 and in following simulations are chosen to be 15 minutes long. Cars can arrive during one time interval and hence would not be connected for the whole time. Therefore, their power connection is determined through (7) where $C_{k_n}^p$ is the connection power of PHEV k at node n , t_l is the interval time length in seconds and $T_{k_n}^A$, $T_{k_n}^D$ are arrival- and departure time in seconds, respectively. In the case where total chargeable energy during one interval exceeds the amount to fully charge/discharge the battery, the maximal power is

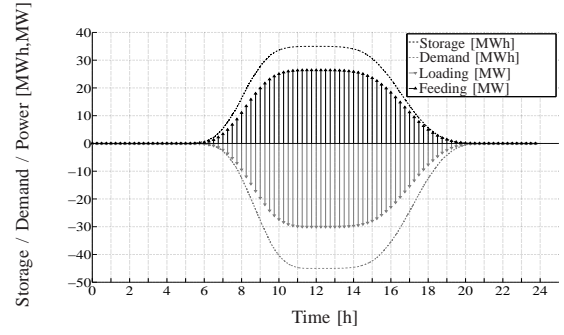


Fig. 4: Presence of PHEVs at hub 2

derived from the SOC, with $C_{k_n}^B$ being the battery capacity. Equation (8) gives the final power connection boundaries.

$$\begin{aligned} \bar{p}_{k_n}^P(t) &= C_{k_n}^p & \forall k_n \in \mathcal{PHEV}_n^P(t) \\ \bar{p}_{k_n}^D(t) &= C_{k_n}^p \frac{T_{k_n}^D - (t-1)t_l}{t_l} & \forall k_n \in \mathcal{PHEV}_n^D(t) \\ \bar{p}_{k_n}^A(t) &= C_{k_n}^p \frac{(t)t_l - T_{k_n}^A}{t_l} & \forall k_n \in \mathcal{PHEV}_n^A(t) \\ \bar{p}_{k_n}^{A,D}(t) &= C_{k_n}^p \frac{T_{k_n}^D - T_{k_n}^A}{t_l} & \forall k_n \in \mathcal{PHEV}_n^A(t) \cup \mathcal{PHEV}_n^D(t) \\ \bar{p}_{k_n}^1(t) &= \frac{(SOC_{k_n}(t) - SOC_{k_n}(t))C_{k_n}^B}{t_l} & \forall k_n \in \mathcal{PHEV}_n(t) \\ \bar{p}_{k_n}^2(t) &= \frac{(SOC_{k_n}(t) - SOC_{k_n}(t))C_{k_n}^B}{t_l} & \forall k_n \in \mathcal{PHEV}_n(t) \end{aligned} \quad (7)$$

$$\begin{aligned} \bar{p}_{k_n}(t) &= \min\{\bar{p}_{k_n}^N(t), \bar{p}_{k_n}^1(t)\} \\ \underline{p}_{k_n}(t) &= \max\{-\bar{p}_{k_n}^N(t), -\bar{p}_{k_n}^2(t)\} \\ &\text{with } \aleph \in \{A, D, P\} \end{aligned} \quad (8)$$

E. Optimal production planning

Production planning is presumed to be performed by a central entity. Here, the Distribution System Operator (DSO) is assumed to assess network security while performing the planning. The DSO considers electricity as well as heat loads of the system and the planned wind infeed based on COSMO-7 ($P_{w,n}^{\Gamma 1}$) forecasts. Total energy costs (9) for the system are minimized by the central entity.

The entire wind production is fed into the system ensuring maximal use of renewable energy generation. This scheme takes into account fixed feed-in tariffs for wind power producers. In case the wind power exceeds system demand, the remaining power is fed into higher network voltage levels through the slack node. Planning errors can be compensated through the slack node, typically done when no or not enough PHEVs are present. The planning algorithm is derived through the optimal power dispatch scheme denoted in (9)-(12). It is independently performed for every time step t in a multi-step optimization. The superscript bc indicates the base case. Equations (10)-(11) denote the system equality constraints expressing that load needs to be met at each hub $i \in \mathcal{H}$ and each node equation needs to be fulfilled at every node $n \in \mathcal{N}$. The inequality constraints in (12) assure that all line capacities $P_{mn}^{bc}(t)$, compressor pressure boost factors $p_{boost,i}^{bc}(t)$, node pressures $p_i^{bc}(t)$, converter inputs $P_{e,i}^{bc}(t)$, $P_{F,i}^{bc}(t)$, $P_{CHP,i}^{bc}(t)$, dispatch factors $\nu_{g,i}^{bc}(t)$ as well as slack node infeeds $P_{e,S}^{bc}(t)$, $P_{g,S}^{bc}(t)$ stay within their predefined limits. Based on this dispatch base system states, such as line flows, etc. are determined.

Minimize

$$f(P_{e,i}(t), P_{g,i}(t)) = \sum_i \pi_e(t) P_{e,i}(t) + \pi_g(t) P_{g,i}(t) \quad (9)$$

subject to

$$\begin{bmatrix} L_{e,i}^{bc}(t) \\ L_{h,i}^{bc}(t) \\ \eta_{ee,i}^{TR} \\ 0 \end{bmatrix} = \begin{bmatrix} \nu_i^{bc}(t) \eta_{ge,i}^{CHP} \\ \nu_i^{bc}(t) \eta_{gh,i}^{CHP} + (1 - \nu_i^{bc}(t)) \eta_{gh,i}^F \end{bmatrix} \begin{bmatrix} P_{e,i}^{bc}(t) \\ P_{g,i}^{bc}(t) \end{bmatrix} \quad (10)$$

$$\begin{aligned} F_{e,m}^{bc}(t) - \sum_{n \in \mathcal{N}_{\setminus \{m\}}} F_{e,mn}^{bc}(t) &= 0 \\ F_{g,m}^{bc}(t) - \sum_{n \in \mathcal{N}_{\setminus \{m\}}} F_{g,mn}^{bc}(t) &= 0 \\ \theta_1^i &= 0 \end{aligned} \quad (11)$$

and

$$\begin{aligned} \underline{P}_{mn}^{bc}(t) &\leq P_{mn}^{bc}(t) \leq \overline{P}_{mn}^{bc}(t) \\ \underline{P}_{boost,i}^{bc}(t) &\leq p_{boost,i}^{bc}(t) \leq \overline{p}_{boost,i}^{bc}(t) \\ \underline{p}_i^{bc}(t) &\leq p_i^{bc}(t) \leq \overline{p}_i^{bc}(t) \\ \underline{P}_{e,i}^{bc}(t) &\leq P_{e,i}^{bc}(t) \leq \overline{P}_{e,i}^{bc}(t) \\ \underline{P}_{F,i}^{bc}(t) &\leq P_{F,i}^{bc}(t) \leq \overline{P}_{F,i}^{bc}(t) \\ \underline{P}_{CHP,i}^{bc}(t) &\leq P_{CHP,i}^{bc}(t) \leq \overline{P}_{CHP,i}^{bc}(t) \\ \underline{P}_{e,S}^{bc}(t) &\leq P_{e,S}^{bc}(t) \leq \overline{P}_{e,S}^{bc}(t) \\ \underline{P}_{g,S}^{bc}(t) &\leq P_{g,S}^{bc}(t) \leq \overline{P}_{g,S}^{bc}(t) \\ \underline{\nu}_{g,i}^{bc}(t) &\leq \nu_{g,i}^{bc}(t) \leq \overline{\nu}_{g,i}^{bc}(t) \\ &\forall i \in \mathcal{H} \\ &\forall m, n \in \mathcal{N} \\ &\forall t \end{aligned} \quad (12)$$

III. BALANCING WIND DEVIATIONS WITH PHEVS

In section II-E, the optimization of the system with the COSMO-7 wind power forecast has been formulated. However, the real wind power production, as described in section II-C will deviate from the planned production, sometimes substantially. Therefore, the PHEVs shall be used for balancing, whenever they are available without sacrificing system security by violating technical constraints. The system state during which the PHEVs are active is clearly dependent on the base case calculated before. In order to investigate the PHEV impact on the system while balancing the wind deviation, the system from figure 1 is reduced to the one depicted in figure 5. The gas network as well as the loads are removed. Hence, the wind power difference $\Delta P_{w,n}$, defined in (17), is here exclusively balanced by PHEVs and the slack node. CHPs are not considered for balancing services. The balancing signal is presumed to be communicated from the proper entity (e.g. the BGR) to the DSO. The base case is considered through net line- and transformer capacities which are here used as constraints. This is achieved by adding or subtracting the base case transformer and line loads to their respective total capacity. The wind power difference needs to be effectively allocated to the connected PHEVs considering their individual SOC and departure time. Two methodologies, a simple heuristic one and one based on model predictive control, are investigated and compared in the following.

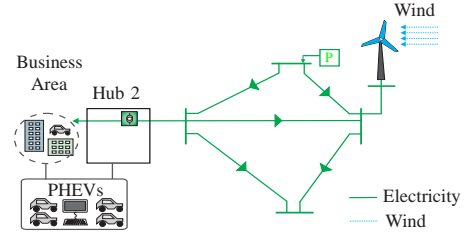


Fig. 5: Network with wind deviation as input

A. Heuristic

One possibility to schedule PHEVs for balancing services dependent on their individual demands can be achieved via heuristics. Heuristics and meta-heuristics are applied for various problems in power systems [21]. Heuristics have the advantage to be fast. However, they do not necessarily find the global optimum. Meta-heuristics have proven to deliver good results in unit commitment problems [22] and have recently been utilized for PHEV scheduling [11]. Heuristic schemes can be useful as the aggregating entity, contracted for balancing services, needs to decide in short time intervals how to control its vehicles optimally or at least with acceptable performance. One possibility could be to sort the connected PHEVs after their SOC. Then, depending whether the balancing power is positive or negative, the vehicle with the highest- or lowest SOC could be scheduled first in order to compensate. This, however, does not take into account when the particular PHEV will actually leave. Hence, a better scheme would account for both aspects. Such a priority list can be expanded depending on the product of individual SOC and departure time. In case of positive wind power deviation the car with the lowest product value will be recharged first. In the other case, when the deviation is negative and the cars need to discharge, simply the one with the highest SOC is scheduled first. Equation (13) summarizes this approach, which does not consider future events.

$$\Delta P_{w,n}(t) = \begin{cases} > 0; & \text{sort ascending } \min\{SOC_{k_n}(t) \cdot T_{k_n}^D\} \\ < 0; & \text{sort descending } \max\{SOC_{k_n}(t)\} \end{cases} \quad (13)$$

$$\forall k_n \in \mathcal{PHEV}_n(t)$$

B. Using MPC for wind balancing with PHEVs

The heuristic method presented in the previous section minimizes the balancing costs only for one time step delivering most likely a suboptimal solution. A different approach is to use available information about the future in order to schedule the PHEVs optimally. An optimization scheme could incorporate known PHEV departure times as well as the more accurate wind forecast COSMO-2 ($P_{w,n}^{\Gamma 2}$) at node n . Here, although computationally demanding, model predictive control (MPC) [23] is used to determine optimal PHEV scheduling. In MPC, an optimization problem is solved using an internal system model to find actions which give the best performance for the system over a predefined time horizon. It is solved using a finite horizon of N predicted time steps in a receding horizon fashion, i.e. at each time step measurements and predictions are performed on which adequate actions of a central controller are based. The problem formulation is derived similar as in [24].

For each time step t an algebraic state vector $\mathbf{z}(t)$ and a dynamic state vector $\mathbf{x}(t)$ can be defined. The algebraic state vector refers to variables derived from the power system state, whereas $\mathbf{x}(t)$ refers to the dynamic state of each PHEV battery considered as storage. Hence, the dynamic state vector is composed of the SOC of all connected PHEVs in t .

$$\begin{aligned} \mathbf{x}(t) &= [\mathbf{SOC}_{k_n}(t)] \\ \forall k_n &\in \mathcal{PHEV}_n(t) \end{aligned} \quad (14)$$

$$\mathbf{z}(t) = [\mathbf{P}_e(t)' \mathbf{P}_g(t)' \Delta \mathbf{P}_w(t)' \theta(t)' \nu_g(t)' \mathbf{p}(t)' \mathbf{p}_{boost}(t)]' \quad (15)$$

where

- $\mathbf{P}_e(t) = [P_{e,1}(t), \dots, P_{e,N_H}(t)]$ are the electricity inputs to the hubs in the balancing case

- $\mathbf{P}_g(t) = [P_{g,1}(t), \dots, P_{g,N_H}(t)]$ are the gas inputs to the hubs in the balancing case

- $\Delta \mathbf{P}_w(t) = [\Delta P_{w,1}(t), \dots, \Delta P_{w,N_N}(t)]$ are the wind power input errors to the system

- $\theta(t) = [\theta_1(t) \dots \theta_{N_N}(t)]$ are the angles of electricity buses in the balancing case

- $\nu(t) = [\nu_1(t) \dots \nu_{N_H}(t)]$ are the dispatch factors of hubs in the balancing case

- $\mathbf{p}(t) = [p_1(t) \dots p_{N_N}(t)]$ are the nodal pressures at gas nodes in the balancing case

- $\mathbf{p}_{boost}(t) = [p_{boost,1}(t) \dots]$ are the compressor boosts.

The control variables at each time step t are defined to include the active PHEV power consumption or supply and the balancing energy drawn from the bulk system.

$$\mathbf{u}(t) = [\mathbf{P}_{e,S}(t)' \mathfrak{P}_n(t)]' \quad (16)$$

Here

- $\mathbf{P}_{e,S}(t)$ denotes the electricity injection from the bulk system

- $\mathfrak{P}_n(t) = [p_{1,n}(t) \dots p_{N_{PHEV_n}}(t)] \forall n \in \mathcal{N}$, where $\mathfrak{P}_n(t)$ denotes the power capacity connections of the connected cars in t at node n according to (7). The additional information on the predicted time horizon is derived from the different forecasts. In the actual time step actions are undertaken that balance the error of the real wind power production $P_{w,n}^R$ and the COSMO-2 forecast $P_{w,n}^{\Gamma 2}$. The information on the future wind production error is derived by the difference between COSMO-2- and COSMO-7 forecast in (17) as, contrary to the latter, COSMO-2 is updated frequently.

$$\begin{aligned} P_{w,n}^R &= [P_{w,n}^R(1), \dots, P_{w,n}^R(T_N)] \\ P_{w,n}^{\Gamma 1} &= [P_{w,n}^{\Gamma 1}(1), \dots, P_{w,n}^{\Gamma 1}(T_N)] \\ P_{w,n}^{\Gamma 2} &= [P_{w,n}^{\Gamma 2}(1), \dots, P_{w,n}^{\Gamma 2}(T_N)] \\ \Delta P_{w,n} &= [P_{w,n}^R(1) - P_{w,n}^{\Gamma 1}(1), P_{w,n}^{\Gamma 1}(2) - P_{w,n}^{\Gamma 2}(2), \\ &\quad \dots, P_{w,n}^{\Gamma 1}(T_N) - P_{w,n}^{\Gamma 2}(T_N)] \end{aligned} \quad (17)$$

Now, the control problem including electricity- and gas network as well as hub equations can be formulated for the system in figure 5 according to (18) with the objective function in (20). Variables indicated with a tilde represent vectors with variable values over the prediction horizon, e.g. $\tilde{\mathbf{u}}(t) = [\mathbf{u}(t), \mathbf{u}(t+1) \dots \mathbf{u}(t+T_N-1)]$. The objective function J is divided into two parts. The first introduces balancing costs of the slack, the second represents costs induced by vehicle scheduling. The slack costs constitute more expensive balancing services $\pi_e^b(t)$, typically paid to the ISO for differing

from the previously submitted schedule. Balancing energy prices are presumed to be known in advance and to be variable [9]. The price could be seen as an incentive from the ISO to provide more PHEV control power during certain periods of the day, e.g. like during nights when the load is low and the fluctuating generation has a large production share.

The vehicle scheduling penalty ensures a reasonable use of the batteries and degradation can be partly avoided. Without these costs the batteries could periodically charge and discharge maintaining the same SOC over the prediction horizon T_N . This penalty is chosen to be magnitudes smaller than the balancing costs in order not to interfere with the main objective. The function enables minimizing expensive balancing power from higher network levels in order to compensate forecast errors [9], [17].

$$\min_{\tilde{\mathbf{u}}(t)} J(\tilde{\mathbf{x}}(t+1), \tilde{\mathbf{z}}(t), \tilde{\mathbf{u}}(t)) \quad (18)$$

subject to

$$\begin{aligned} \tilde{\mathbf{x}}(t+1) &= \tilde{\mathbf{f}}(\tilde{\mathbf{x}}(t), \tilde{\mathbf{z}}(t), \tilde{\mathbf{u}}(t)) \\ \tilde{\mathbf{g}}(\tilde{\mathbf{x}}(t), \tilde{\mathbf{z}}(t), \tilde{\mathbf{u}}(t)) &= 0 \\ \tilde{\mathbf{h}}(\tilde{\mathbf{x}}(t), \tilde{\mathbf{z}}(t), \tilde{\mathbf{u}}(t)) &\leq 0 \end{aligned} \quad (19)$$

with

$$\begin{aligned} J &= \sum_{t=1}^{t_N} \sum_{n=1}^{N_N} \{ \text{sign}[\Delta P_{w,n}(t)] (\pi_e^b(t) P_{e,S}(t)) \\ &\quad + \text{sign}[\sum_{k_n}^{N_{PHEV_n}} p_{k_n}(t)] \pi_e^{PE}(t) \sum_{k_n}^{N_{PHEV_n}} p_{k_n}(t) \} \end{aligned} \quad (20)$$

and

$$\tilde{P}_{mn}^*(t) \leq \tilde{P}_{mn}(t) \leq \tilde{P}_{mn}^*(t) \quad (a)$$

$$\tilde{p}_{boost,i}^*(t) \leq \tilde{p}_{boost,i}(t) \leq \tilde{p}_{boost,i}^*(t) \quad (b)$$

$$\tilde{p}_i^*(t) \leq \tilde{p}_i(t) \leq \tilde{p}_i^*(t) \quad (c)$$

$$\tilde{P}_{e,i}^*(t) \quad \forall i \neq 2 \quad = \quad 0 \quad (d)$$

$$-\Delta \tilde{P}_{w,n}(t) \leq \sum_{k_n}^{N_{PHEV_n}} \tilde{p}_{k_n}(t) \leq \Delta \tilde{P}_{w,n}(t) \quad (e)$$

$$\tilde{P}_F^*(t) \leq \tilde{P}_F(t) \leq \tilde{P}_F^*(t) \quad (f)$$

$$\tilde{P}_{CHP}^*(t) \leq \tilde{P}_{CHP}(t) \leq \tilde{P}_{CHP}^*(t) \quad (g)$$

$$\tilde{P}_{e,S}^*(t) \leq \tilde{P}_{e,S}(t) \leq \tilde{P}_{e,S}^*(t) \quad (h)$$

$$\tilde{P}_{g,S}^*(t) \leq \tilde{P}_{g,S}(t) \leq \tilde{P}_{g,S}^*(t) \quad (i)$$

$$\tilde{v}_{g,i}^*(t) \leq \tilde{v}_{g,i}(t) \leq \tilde{v}_{g,i}^*(t) \quad (j)$$

$$\tilde{SOC}_{k_n}^A(t^A) \leq SOC_{k_n}(t^A) \leq \tilde{SOC}_{k_n}^A(t^A) \dots (k) \quad \forall k_n \in \mathcal{PHEV}_n^A(t)$$

$$\tilde{SOC}_{k_n}(t) \leq SOC_{k_n}(t) \leq \tilde{SOC}_{k_n}(t) \dots (l) \quad \forall k_n \in \mathcal{PHEV}_n^D(t) \cup \mathcal{PHEV}_n^P(t)$$

$$\tilde{p}_{k_n}(t) \leq \tilde{p}_{k_n}(t) \leq \tilde{p}_{k_n}(t) \dots (m) \quad \forall k_n \in \mathcal{PHEV}_n(t)$$

$$\forall n \in \mathcal{N}$$

$$\forall i \in \mathcal{H}$$

$$\forall t$$

(21)

Equation (21) gives an overview of the system inequality constraints including wind infeeds and PHEV power balancing and can be derived from (12). Here, the constraints with a

star as superscript denote variables where the actual borders are constructed from their particular capacities and the base case loading, e.g. $\tilde{P}_{mn}^*(t) = \tilde{P}_{mn}(t) - \tilde{P}_{mn}^{bc}(t)$. The tilde again indicates a constraint vector over the prediction horizon. Constraint (21)(d) denotes that the electric power consumption at all but hub number 2 has to be zero. Recall that the PHEVs are connected to hub number 2, only. Constraint (21)(e) indicates that the total PHEV power consumption or production is maximally compensating the introduced forecast error defined in (17). Constraint (21)(k) assures that the SOC at arrival, denoted by superscript A , of all PHEVs is considered in the respective time step as the starting value for all following steps within T_N . The SOC of already parked or departing PHEVs is considered in constraint (21)(l). It is bounded between the maximal and minimal possible SOC. Lastly, the power of each PHEV in each time step t is bounded through constraint (21)(m) taking into account (7) and the three sets of $\mathcal{PHEV}_n(t)$.

IV. CASE STUDIES COMPARING THE MPC- AND THE HEURISTIC METHOD

The performance of the two algorithms described in III-A and III-B is compared in the following case studies. The base loads as well as energy carrier- and balancing energy prices for the period under investigation are presumed to be constant and known. The focus is laid upon balancing the error introduced by renewable energy generation. In order to compare the results of both methods with the global optimal solution, the scheme in III-B can be employed with complete information, e.g. the COSMO-2 information is substituted by the actual real wind speeds, i.e. power $P_{w,n}^R$. In such a case, in which the future is completely known, the allocation of energy to the cars can be optimally computed. The results of the optimal solution can be used as reference point to estimate the quality of the results of the other algorithms.

A. Study 1: Small PHEV number, simple PHEV time schedules and simple wind data

In this example, a comparison between the heuristic and the MPC algorithm is performed using complete information. The study is conducted for ten PHEVs. Cars 1-5 are fully depleted at their arrival (i.e. SOC=20%) whereas cars 6-10 are fully charged. All ten cars are present from the beginning of the time interval. PHEV 1-5 stay parked and connected for the whole prediction horizon. PHEV 6-10 leave after one hour. The system is simulated including the following presumptions:

- $T_N = 12$ (i.e. 3 hours)
- $\Delta P_{w,2}(t) = 0$ in $t = 1 - 4$
- $\Delta P_{w,2}(t) < 0$ for $t = 5 \dots T_N$
- Constant balancing energy prices ($\pi_e^b = \text{const}$)

Obviously, this situation poses a worst case scenario for both schemes since all PHEV resources are either at their lower- or upper bound, the PHEVs which would be capable of supplying balancing services leave exactly at the time when their services are demanded and the overall forecast error is negative. The result of the heuristic is visualized in figure 6 whereas the

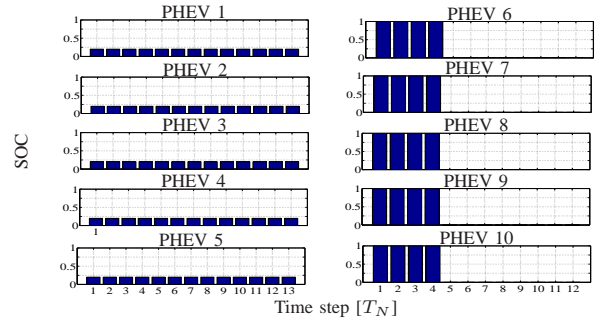


Fig. 6: Study 1: SOC calculated with the heuristic

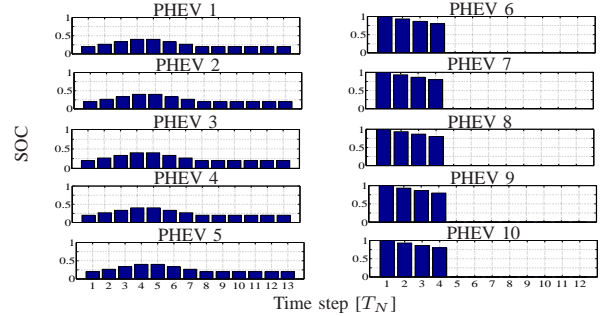


Fig. 7: Study 1: SOC calculated using MPC with complete information

MPC schemes is shown in figure 7. Both figures plot the SOC of the vehicles over the prediction horizon. Figure 6 clearly illustrates the disadvantage of the heuristic method in such extreme cases. The future, i.e. $\Delta P_{w,2}(t=2) \dots \Delta P_{w,2}(T_N)$, is not taken into account at all. After $t = 4$ PHEV 6-10 leave and the following negative wind error cannot be compensated through the PHEVs apparent because their batteries are fully depleted. Hence, balancing services need to be fully performed by the slack node. On the other hand, the MPC approach does consider the future production. The scheme distributes available power from cars 6-10 to cars 1-5 as long as no balancing services are demanded. Clearly, this redistribution of energy under PHEVs impacts the low voltage network and introduces battery losses. However, they are both not considered here. The redistribution takes the respective power connections of the PHEVs according to (7) and (21) fully into account. The results are shown in figure 7, which indicates that PHEV 1-5 are recharged throughout time steps 1-4 to be utilized for balancing services during the later time steps. Hence, the PHEVs can offer balancing power after $t = 4$ reducing total balancing costs. The computation time was found to be 90 times higher for the optimization.

B. Study 2: Small PHEV fleet and real wind data

This study shows a realistic example and compares both schemes. It is conducted with 60 PHEVs and for 12 time steps. The wind power $P_{w,2}^{\Gamma 1}$ forecasted by COSMO-7 is shown in figure 8a. During the first 6 time steps the wind speed is forecasted to be not sufficient for power production. The calculated wind power using actually measured wind speed is shown in figure 8b. Obviously, the wind speed increased sooner than forecasted therefore the power production deviates

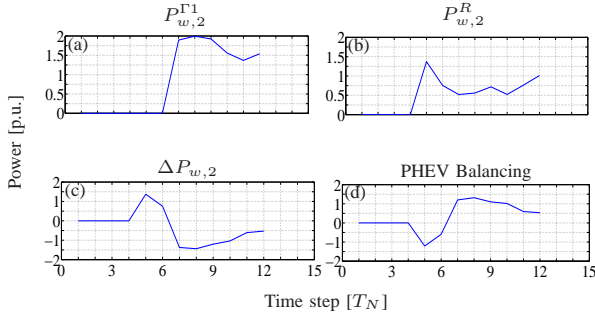


Fig. 8: Study 2: Resulting powers using the heuristic: (a) COSMO-7 forecast, (b) real wind (c) wind deviation (d) PHEV balancing power

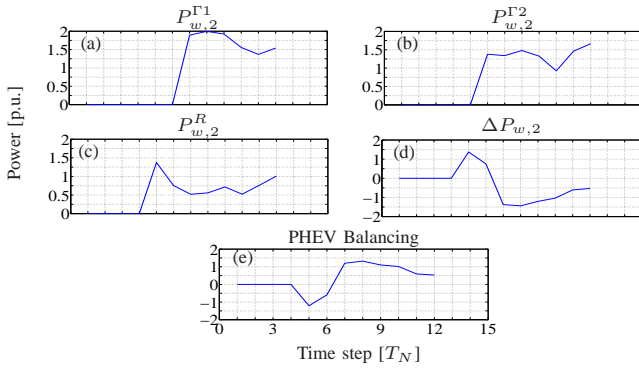


Fig. 9: Study 2: Resulting powers using the MPC with COSMO-2 ($P_{w,2}^{\Gamma 2}$): (a) COSMO-7 forecast, (b) COSMO-2, (c) real wind (d) wind deviation (e) PHEV balancing power

in time step 4 and the following from the forecasted. This forecast error is depicted in figure 8c. The balancing behavior of the PHEVs is depicted in figure 8d. Clearly, the heuristic finds a good solution in this case as almost all of the demanded balancing power is supplied by the PHEVs.

Figure 9 shows the solution which the MPC algorithm delivers. Figures 9a and 9b depict the COSMO-7 forecast $P_{w,2}^{\Gamma 1}$ and the COSMO-2 forecast $P_{w,2}^{\Gamma 2}$, respectively. Here as well, COSMO-2 provides a more accurate forecast than COSMO-7. Figure 9c displays the real wind power production $P_{w,2}^R$ and figure 9d shows the wind production error. The resulting balancing behavior is shown in figure 9e. It depicts the same PHEV balancing as found in 8d. Obviously, the MPC algorithm and the heuristic deliver the same PHEV balancing behavior since the resulting total PHEV balancing power is the same in both cases (i.e. fig. 8d and fig. 9e). However, the methods do differ in the actual, individual PHEV set points of energy consumption. Here, as the goal is to fully balance the error, both are capable of finding this optimal solution, since the slack is not utilized at all. The heuristic scheme is capable of delivering the global optimum although less information is utilized, e.g. no second forecast (COSMO-2) is used. It is easily understood that it finds the optimal solution because enough balancing power is available and no worst case scenario is apparent. The batteries are not at their respective bounds during the balancing interval, i.e. their

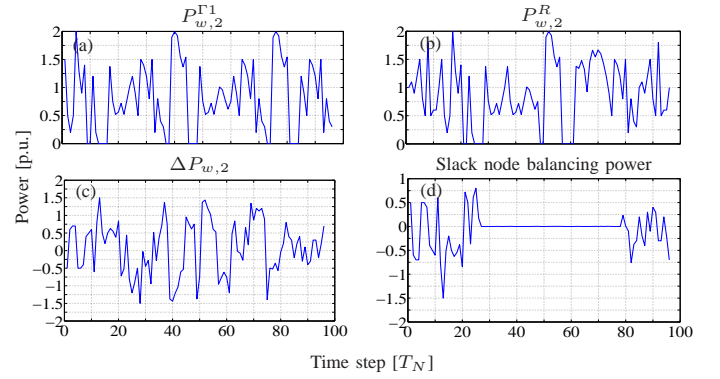


Fig. 10: Study 3: Resulting powers using the heuristic: (a) COSMO-7 forecast, (b) real wind (c) wind deviation (d) slack node balancing power

batteries are neither completely full nor empty. The more cars are connected and the less power is to be balanced (i.e. the forecast is not completely off), the more flexible is the heuristic method in its scheduling algorithm, balancing the production planning error completely. Here, the heuristic method clearly is more advantageous since it delivers the same result in terms of minimizing slack node utilization but with lower computational efforts.

C. Study 3: Large PHEV fleet and real wind data

This example discusses balancing services of a PHEV fleet with a large number of cars. Here, in contrary to the former case studies, 7000 are utilized. Clearly, more balancing power can then be supplied to the system. The time horizon is chosen to be a full day (96 time steps). The departure times as well as the arrival times correspond to the behavior discussed in section II-D. The system load, electric- as well as heat load is assumed to be higher during the day than during night. It is not depicted here. Whenever the wind power production is larger than total system demand the power is fed back to the bulk system through the slack node. During the first 20 time steps PHEVs are not connected to the system. The wind deviation (fig. 10c) resulting from the COSMO-7 forecast (fig. 10a) and the actual production (fig. 10b) is fully compensated through the slack node as visualized in figure 10d. Shortly after time step 28 more and more PHEVs are connecting and are available for balancing services. Until time step 75 enough balancing power from the PHEVs is provided to completely compensate the planning error. Hence, balancing services by the slack node are not demanded. Then, the cars leave from work lowering total offered balancing power to a level that only allows for partial production error compensation.

The MPC algorithm does not deliver results for this case as memory constraints are violated. It can only be employed for cases with large numbers of distributed storages when aggregating them intelligently. Here, a big advantage of the heuristic method is accentuated. This algorithm finds quickly a solution likely close to the global minimum in terms of forecast error correction. For practical cases, where wind errors lie in the region of MWs and large numbers of PHEVs need to be employed, it can easily be utilized. However, no

attention has been paid here to investigate the maximal error possible to be corrected by the PHEV fleet.

V. SUMMARY AND OUTLOOK

This paper introduces an approach to supply balancing power for stochastic wind generation using a large number of PHEVs. Wind generation planning is based on a long term forecast COSMO-7. The balancing of the forecast error is managed using two different approaches. Here, a heuristic based on individual SOC as well as departure time of PHEVs and MPC are introduced and discussed. The latter method uses the short term forecast COSMO-2 to plan storage utilization more adequately. The PHEVs are presumed to be fully available for balancing services and individual transportation goals are neglected. It has been shown that the heuristic is able to find the optimal solution in terms of error balancing if the PHEVs are neither fully charged or discharged. MPC, used as a reference has been shown to deliver the optimal solution when not managing large numbers of cars and prediction steps. However, it is shown that both approaches can manage the PHEVs possibly reducing balancing costs in the future. Clearly, PHEVs offers a means to regulate the wind power in future systems.

VI. ACKNOWLEDGEMENTS

The work is sponsored by the ETH Zurich (Swiss Federal Institute of Technology Zurich) under research grant TH 2207-3. The authors would like to thank all colleagues, especially A. Ulbig and E. Iggland at the power systems laboratory (PSL) at ETH Zurich for helpful discussions.

REFERENCES

- [1] European Commission. Impact assessment on the EU's objectives on climate change and renewable energy. Technical report, 2008.
- [2] Euractiv.com. <http://www.euractiv.com/en/energy/eu-renewable-energy-policy/article-117536>.
- [3] European Commission. Proposal for a directive on the promotion of the energy from renewable sources. Technical report, 2008.
- [4] Hannes Weigt. Germany's wind energy: the potential for fossil capacity replacement and cost saving. *Applied Energy*, 86(10):1857–1863, 2009.
- [5] W. Buenger U., Leonhard. Energiespeicher im stromversorgungsnetz mit hohem anteil an erneuerbarer energietraeger. Technical report, VDE, 2008.
- [6] ETG. Smart Distribution 2020 - Virtuelle Kraftwerke in Verteilungsnetzen. Technical report, VDE (German Society of Electrical Engineers), 2008.
- [7] Thomas H. Bradley and Andrew A. Frank. Design, demonstrations and sustainability impact assessments for plug-in hybrid electric vehicles. *Renewable and Sustainable Energy Reviews*, 13(1):115–128, 2009.
- [8] W. Kempton and J. Tomic. Vehicle-to-grid power implementation: From stabilizing the grid to supporting large-scale renewable energy. *Journal of Power Sources*, 144(1):280–294, 2005.
- [9] S. L. Andersson, A. K. Eloffsson, M. D. Galus, L. Göransson, S. Karlsson, F. Johnsson, and G. Andersson. Plug-in hybrid electric vehicles as regulating power providers: Case studies of Sweden and Germany. *Energy Policy*, 2010.
- [10] C. Guille and G. Gross. A conceptual framework for the vehicle-to-grid (v2g) implementation. *Energy Policy*, 37(11):4379–4390, 2009.
- [11] Ahmed Yousuf Saber and Ganesh Kumar Venayagamoorthy. Intelligent unit commitment with vehicle-to-grid –a cost-emission optimization. *Journal of Power Sources*, 195(3):898–911, 2010.
- [12] M. Geidl and G. Andersson. Optimal power flow of multiple energy carriers. *IEEE Transactions on Power Systems*, 22(1):145–155, 2007. 0885-8950.

- [13] A. J. del Real, M. D. Galus, C. Bordons, and G. Andersson. Optimal power dispatch of energy networks including external power exchange. In *European Control Conference (ECC) 09*, pages 1–6, Budapest, Hungary, 2009.
- [14] M. D. Galus and G. Andersson. Integration of plug-in hybrid electric vehicles into energy systems. In *Powertech 09*, Bucharest, Romania, 2009.
- [15] Steppeler J. Doms, G. Meso-gamma scale forecasts using the non-hydrostatic model Im. *Meteorology and Atmospheric Physics*, 82(1-2):75–96, 2003.
- [16] METEOSwiss. <http://www.meteoschweiz.admin.ch/web/de/wetter/modelle/cosmo.html>.
- [17] Y. G. Rebours, D. S. Kirschen, M. Trotignon, and S. Rossignol. A survey of frequency and voltage control ancillary services - part ii: Economic features. *IEEE Transactions on Power Systems*, 22(1):358–366, 2007. 0885-8950.
- [18] M. D. Galus and G. Andersson. Demand management for grid connected plug-in hybrid electric vehicles (phev). In *IEEE Energy 2030*, pages 1–8, Atlanta, GA, USA, 2008.
- [19] M. D. Galus and G. Andersson. Power system considerations of plug-in hybrid electric vehicles based on a multi energy carrier model. In *Power and Energy Society (PES) General Meeting*, Calgary, Canada, 2009.
- [20] A. Heider and H. J. Haubrich. Impact of wide-scale ev charging on the power supply network. In *IEE Colloquium on Electric Vehicles - A Technology Roadmap for the Future (Digest No. 1998/262)*, pages 6/1–6/4, 1998.
- [21] K. Y. Lee and M. A. El-Sharkawi. *Modern Heuristic Optimization Techniques: Theory and Applications to Power Systems*. 2008.
- [22] T. Senjyu, K. Shimabukuro, K. Uezato, and T. Funabashi. A fast technique for unit commitment problem by extended priority list. *IEEE Transactions on Power Systems*, 18(2):882–888, 2003. 0885-8950.
- [23] Bordons C. Camacho, E.F. *Model Predictive Control*. Springer, New York, 2004.
- [24] M. Arnold, R. Negenborn, G. Andersson, and B. De Schutter. Model based predictive control applied to multi energy carrier systems. In *IEEE Power and Energy Society General Meeting (PES)*, Calgary, Canada, 2009.



Matthias D. Galus was born in Swientochlowitz, Poland. He received a Dipl.-Ing. degree in electrical engineering and a Dipl.-Ing. degree in industrial engineering from the RWTH Aachen, Germany, in 2005 and in 2007, respectively. He joined the Power Systems Laboratory of ETH Zurich, Switzerland in 2007 where he is working towards a PhD. His research is dedicated to modeling, optimization and efficient integration of PHEV into power systems. He is a student member of the IEEE and VDE (German society of electrical engineers).



Raffael La Fauci was born in Zürich, Switzerland. He received his B.Sc. in electrical engineering from the ETH Zurich (Swiss Federal Institute of Technology) in 2009. Currently, he is working toward his M.Sc. degree with Major in Electrical Power Systems and Mechatronics. He is a student member of the IEEE.



Göran Andersson was born in Malmö, Sweden. He obtained his MSc and PhD degree from the University of Lund in 1975 and 1980, respectively. In 1980 he joined ASEA, now ABB, HVDC division in Ludvika, Sweden, and in 1986 he was appointed full professor in electric power systems at the Royal Institute of Technology (KTH), Stockholm, Sweden. Since 2000 he is full professor in electric power systems at ETH Zurich, Switzerland, where he heads the Power Systems Laboratory. His research interests are in power system analysis and control, in particular power system dynamics and issues involving HVDC and other power electronics based equipment. He is a member of the Royal Swedish Academy of Engineering Sciences and Royal Swedish Academy of Sciences and a Fellow of IEEE.